

## A TWO-TEMPERATURE ACCRETION DISK MODEL FOR CYGNUS X-1: STRUCTURE AND SPECTRUM

STUART L. SHAPIRO AND ALAN P. LIGHTMAN

Center for Radiophysics and Space Research, Cornell University\*

AND

DOUGLAS M. EARDLEY

Physics Department, Yale University†

Received 1975 May 5; revised 1975 August 4

### ABSTRACT

We present a model for Cygnus X-1, involving an accretion disk around a black hole, which can explain the observed X-ray spectrum from 8 to 500 keV. In particular we construct a detailed model of the structure of an accretion disk whose inner region is considerably hotter and geometrically thicker than previous disk models. The inner region of the disk is optically thin to absorption, is gas-pressure dominated, and yields, from first principles, electron temperatures of  $10^9$  K and ion temperatures 3–300 times hotter. The spectrum above 8 keV is produced by inverse Compton scattering of soft X-ray photons in the two-temperature inner region of the disk. This spectrum is computed by numerical integration of the Kompane'ts equation, modified to account for escape of photons from a region of finite (order unity) electron scattering optical depth.

*Subject headings:* radiative transfer — stars: black holes — X-rays: sources

### I. INTRODUCTION

Current estimates of the mass of the compact X-ray source Cyg X-1 give  $M \gtrsim 10 M_{\odot}$  (Paczynski 1974; Avni and Bahcall 1975), indicating that this object is the most likely candidate for a black hole. If Cyg X-1 contains a black hole, the observed X-rays would originate from the inner portion of an accretion disk surrounding the black hole. The disk would be formed from gas captured from the companion star of the binary system, HDE 226868. One of the most important requirements of this (or any other) model is that it reproduce the observed X-ray spectrum. In this paper we present detailed calculations of the structure and spectrum of an accretion disk around a black hole which yield a close fit to the observations of Cyg X-1. A summary of our results has previously appeared (Eardley *et al.* 1975).

Historically, the "cool disk model" proposed to explain accretion onto a black hole in a close binary system (Pringle and Rees 1972; Shakura and Sunyaev 1973; Novikov and Thorne 1973) was found to be incapable of producing the observed, hard X-rays ( $\sim 100$  keV) from Cyg X-1 (Lightman and Shapiro 1975). Thorne and Price (1975) demonstrated that *if* the inner portion of an accretion disk consisted of optically thin, high-temperature gas ( $\sim 10^9$  K) instead of the optically thick, low-temperature gas characterizing the cool disk model, *then* the observed hard component of the Cyg X-1 spectrum near 100 keV could be explained. They argued that the secular instability present in the cool disk inner region (Lightman and Eardley 1974) could swell this optically thick, radiation-pressure dominated region to a hot, gas-pressure dominated, optically thin region. Their model, though semiempirical, suggested how the observational data for Cyg X-1 and the accretion disk model might be reconciled.

The main result of this paper is that the cool disk model is not unique. There exists a second, much hotter, self-consistent solution for an accretion disk around a black hole, with the same boundary conditions. When applied to Cyg X-1, this solution yields from first principles the required thermal emission temperatures of  $10^9$  K and is able to reproduce the observed X-ray spectrum above  $\sim 8$  keV. The disk in Cyg X-1 would choose the hot rather than the cool disk structure, if the cool one is secularly unstable. In § II we discuss the physical conditions that must exist in the disk to explain the observed spectrum from Cyg X-1. In § III we describe the detailed structure of and spectrum from the hot, inner portion of the disk. In § IV the results of numerical studies of the proposed two-fluid accretion disk model are presented and analyzed.

### II. PHYSICAL CONDITIONS IN THE DISK AROUND CYGNUS X-1

It is useful to describe, independently of specific cooling mechanisms and spectral considerations, the physical conditions in an accretion disk around a black hole which are necessary to explain the observations of Cyg X-1. These conditions provide strong motivation for the model we shall construct.

\* Supported in part by the National Science Foundation Grant MPS 05056-A02.

† Supported in part by the National Science Foundation (GP-36317).

a) *Disk Temperature Range*

The maximum and minimum temperatures achievable in the disk are determined by the extreme limiting cases of (1) complete internalization of gravitational energy by an optically thin gas ( $T \rightarrow T_{\max}$ ) and (2) LTE in an optically thick gas ( $T \rightarrow T_{\min}$ ). From the flux,  $F$ , emitted by any accretion disk around a nonrotating black hole (independent of the details of vertical structure) at the radius  $r$  (Shakura and Sunyaev 1973), we may write

$$\frac{1}{4}aT_{\min}^4(r) = F(r) = \left(\frac{3}{8}\pi\right)\dot{M}(GM/r^3)\mathcal{J}, \quad (1a)$$

or

$$T_{\min} \sim 3 \times 10^6 \text{ K} (M/10 M_{\odot})^{-1/2} (\dot{M}/6 \times 10^{17} \text{ g s}^{-1})^{1/4}, \quad (1b)$$

where  $M$  and  $\dot{M}$  are the mass of the black hole and mass accretion rate, respectively,  $a$  is the radiation constant, and  $\mathcal{J} \equiv 1 - (6GM/rc^2)^{1/2}$ . In equation (1b), the flux has been evaluated at the point of maximum emission at  $r_m \approx 10 GM/c^2$ , and  $M$  and  $\dot{M}$  have been normalized to values appropriate for Cyg X-1. The low value of  $T_{\min}$  explains why the optically thick, cool disk model fails for Cyg X-1. For mass accretion rates near the Eddington limit, the inner region of the cool disk becomes optically thin and approaches temperatures of  $4 \times 10^8$  K. However, the predicted flux in the observable X-ray band is far too high (see Shakura and Sunyaev 1973, Lightman and Shapiro 1975, for details). For rapidly rotating holes, with the appropriate X-ray luminosity, disk models can have an emission temperature larger than  $10^8$  K, but not as large as  $10^9$  K (Thorne and Price 1975).

The temperature  $T_{\max}$  is determined by the gravitational binding energy of an ion at the inner edge of the disk at  $r_1 = 6GM/c^2$ . Thus,

$$kT_{\max} \sim GMm_p/r_1 = \frac{1}{6}m_p c^2, \quad (2a)$$

or

$$T_{\max} \sim 2 \times 10^{12} \text{ K}. \quad (2b)$$

Temperatures approaching  $T_{\max}$  characterize the fluid near the event horizon in the case of optically thin, spherically symmetric accretion (Shvartsman 1971; Shapiro 1974). The observations indicate that the hottest emission temperature from Cyg X-1,  $T \sim 10^9$  K, lies between  $T_{\min}$  and  $T_{\max}$ , assuming thermal emission. We of course cannot rule out alternative models in which a very different temperature, or no temperature at all, characterizes the emitting electrons; but we judge these possibilities to be less likely.

b) *The Temperature-dependent Disk Structure*

Without considering cooling mechanisms, one can determine the disk structure in terms of the ion and electron temperatures,  $T_i$  and  $T_e$  (which may not be equal). From observations, one can infer an electron temperature, assuming the emission is thermal. Then, assuming  $T_i \geq T_e$ , we can determine the allowable range of the physical variables which describe the emitting region. Three of the principal equations which describe this hot, inner portion of a (Newtonian) disk composed of pure hydrogen are:

*hydrostatic equilibrium:*

$$P/h = \rho(GM/r^3)h; \quad (3)$$

*angular momentum conservation:*

(viscous stress) · (area) ·  $r$  = (angular momentum per unit mass) · (mass accretion rate), or

$$(\alpha P)(2\pi r \cdot 2h)r = (GMr)^{1/2} \dot{M} \mathcal{J}; \quad (4)$$

*equation of state:*

$$P = \rho k(T_i + T_e)/m_p. \quad (5)$$

In the above equations  $P$ ,  $\rho$ ,  $T_i$ ,  $T_e$ , and  $h$  are the pressure, density, ion and electron temperatures, and the disk half-thickness, respectively. In equation (4) the usual viscosity law has been assumed, i.e., shear stress =  $\alpha P$  ( $0.01 \leq \alpha \leq 1$  [see Shakura and Sunyaev 1973; Eardley and Lightman 1975]). The angular momentum per unit mass for gas in nearly circular Keplerian orbits is  $(GMr)^{1/2}$ , and  $\mathcal{J}$  expresses the boundary condition that the viscous stress must vanish at the inner edge of the disk,  $r = r_1$ . The dominant pressure source is assumed to be gas pressure, which we verify below. Two additional equations, one which determines the coupling between ions and electrons in the plasma and the other which determines the electron temperature through radiative cooling, will be specified in § III. Without these additional equations, equations (3)–(5) can be solved as a function of  $T_i$  and

$T_e$ . Equations (3)–(5) may be found in Shakura and Sunyaev (1973) for the case  $T_i = T_e$ . Solving the equations, we obtain:

$$h = (6 \times 10^3 \text{ cm}) M_* r_*^{3/2} \left( \frac{T_i + T_e}{10^9 \text{ K}} \right)^{1/2}, \quad (6a)$$

$$\rho = (0.5 \text{ g cm}^{-3}) M_*^{-2} r_*^{-3} \dot{M}_* \mathcal{J} \alpha^{-1} \left( \frac{T_i + T_e}{10^9 \text{ K}} \right)^{-3/2}, \quad (6b)$$

$$P = (4 \times 10^{17} \text{ dyn cm}^{-2}) M_*^{-2} r_*^{-3} \dot{M}_* \mathcal{J} \alpha^{-1} \left( \frac{T_i + T_e}{10^9 \text{ K}} \right)^{-1/2}, \quad (6c)$$

where  $M_* \equiv M/3 M_\odot$ ,  $\dot{M}_* \equiv \dot{M}/10^{17} \text{ g s}^{-1}$ , and  $r_* \equiv r/(GM/c^2)$ .

From equations (6) and (1a), we may compute three important quantities: the ratio of radiation to gas pressure in the disk,  $P_R/P$ ; the optical depth to free-free absorption measured from the disk midplane to the surface,  $\tau_*$ ; and the electron-scattering optical depth from the disk midplane to the surface,  $\tau_{\text{es}}$ . Since the dominant source of opacity is electron scattering, radiation pressure perpendicular to the disk plane is given by  $P_R \sim F\tau_{\text{es}}/c$ , where

$$\tau_{\text{es}} = \kappa_{\text{es}} \rho h = (1 \times 10^3) M_*^{-1} r_*^{-3/2} \dot{M}_* \mathcal{J} \alpha^{-1} \left( \frac{T_i + T_e}{10^9 \text{ K}} \right)^{-1}, \quad (7a)$$

and where  $\kappa_{\text{es}} = 0.38 \text{ cm}^2 \text{ g}^{-1}$  is the scattering opacity. Thus, the ratio  $P_R/P$  is given by

$$P_R/P \approx \frac{F\tau_{\text{es}}/c}{\rho\kappa(T_i + T_e)/m_p} = 30 M_*^{-1} r_*^{-3/2} \dot{M}_* \mathcal{J} \left( \frac{T_i + T_e}{10^9 \text{ K}} \right)^{-1/2}. \quad (7b)$$

The absorption optical depth is given by

$$\tau_* = (\kappa_{\text{es}} \bar{\kappa}_{\text{ff}})^{1/2} \rho h = (7 \times 10^{-2}) M_*^{-2} r_*^{-3} \dot{M}_*^{3/2} \mathcal{J}^{3/2} \alpha^{-3/2} \left( \frac{T_e}{10^9 \text{ K}} \right)^{-7/2} \left( 1 + \frac{T_i}{T_e} \right)^{-7/4}, \quad (7c)$$

where  $\bar{\kappa}_{\text{ff}} = 6 \times 10^{23} \rho T_e^{-7/2}$  is the Rosseland mean opacity for free-free absorption.

If the observed, hard X-rays from Cyg X-1 originate from the inner portion of an accretion disk with  $T_e \geq 10^9 \text{ K}$ , then equation (7b), evaluated at typical radii, implies that gas pressure dominates radiation pressure in that region. Equation (7c) indicates that this region is optically thin to absorption, since  $\tau_* \ll 1$ . Finally, equation (7a) shows that the inner portion of the disk may be marginally thick to electron scattering, since  $\tau_{\text{es}} \lesssim 1$  for  $T_i \gg T_e$ . In general, therefore, the observations of Cyg X-1 require the inner portion of an accretion disk about a central black hole to be optically thin to free-free absorption, and gas-pressure dominated. The consequences of this conclusion are explored further in the following sections.

### c) The Two-Temperature Requirement

In steady-state the electron heating and cooling rates must be equal. Since the medium is optically thin to absorption, the electron cooling rate,  $\Lambda_e$ , can be expressed as:

$$\Lambda_e = (5.2 \times 10^{20} \rho^2 T_e^{1/2}) A_{\text{ff}} \text{ ergs s}^{-1} \text{ cm}^{-3}, \quad (8)$$

where the term in parentheses is the bremsstrahlung cooling rate and the multiplying factor  $A_{\text{ff}}$  allows for possible additional cooling processes, i.e.,  $A_{\text{ff}} \geq 1$ .

The heating rate, arising from gravitational and viscous energy release, is  $F/h$  (ergs s<sup>-1</sup> cm<sup>-3</sup>). Equating the two rates and using equations (1a), (6a, b), and (8), we find

$$\left( 1 + \frac{T_i}{T_e} \right)^{5/4} \left( \frac{T_e}{10^9 \text{ K}} \right)^{3/4} = 20 A_{\text{ff}}^{1/2} M_*^{-1/2} r_*^{-3/4} \dot{M}_*^{1/2} \mathcal{J}^{1/2} \alpha^{-1}. \quad (9)$$

If  $T_e \sim 10^9 \text{ K}$  in the inner portion of the disk, we find from equation (9) that  $T_i > T_e$ . A one-temperature solution to the structure equations may exist for the inner region, but the required temperature  $T_e = T_i$  exceeds  $10^{10} \text{ K}$ , as shown from equation (9), and is inconsistent with the simplest interpretation of the observations. (New radiative processes are important at  $10^{10} \text{ K}$ , such as pair production/annihilation, which we have not tried to compute. These processes increase the cooling rate, i.e., increase  $A_{\text{ff}}$ ; so by equation (9),  $T_e$  must be even greater, further increasing the cooling rate, and so on. Whether a one-temperature solution exists at all is an open question.) Thus, the observations of Cyg X-1 indicate that in the inner portion of the accretion disk, the ion temperature exceeds the electron temperature.

If the mechanism of viscous dissipation in the disk puts most of the heating into the ion population, then  $T_i$  will naturally exceed  $T_e$ . Subsonic turbulent viscosity will probably do this; supersonic turbulence, or ohmic losses which accompany magnetic reconnection, probably will not. However, even if the electrons and ions are heated equally, the electrons can cool much more efficiently, so that for a given mass element,  $T_i$  will substantially exceed  $T_e$  most of the time. Our calculations below, which presume  $10^9 \text{ K} \sim T_e < T_i \sim 10^{10-11} \text{ K}$ , will therefore be valid "most of the time" even for this case (see Shapiro and Salpeter 1975 for a rather similar situation involving accretion onto neutron stars). Then about half of the total luminosity would emerge from the disk as an inverse Compton spectrum at  $T_e \sim 10^9 \text{ K}$ , as discussed below; whereas the other half would emerge as brief, intense "flashes" of radiation, as electrons quickly cool from  $\sim T_i$  to  $\sim 10^9 \text{ K}$ . These flashes might appear as  $\gamma$ -rays between 100 keV and 10 MeV if (relativistic) inverse Compton cooling and free-free emission dominate the cooling or at softer energies near  $\lesssim 10 \text{ keV}$  if synchrotron radiation is significant. We will not attempt to calculate these effects.

### III. STRUCTURE OF THE TWO-TEMPERATURE DOMAIN

#### a) Basic Assumptions and Equations

Applying the results reached above, we construct from first principles a modified accretion disk model which can explain the observed, hard X-ray spectrum of Cyg X-1. The key assumptions which determine the structure of the inner portion of the disk are:

1. The dominant pressure source is gas pressure ( $P \gg P_R$ ).
2. The gas is optically thin to absorption ( $\tau_* \ll 1$ ).
3. The ions and electrons are coupled by collisional energy exchange, and those plasma instabilities which could provide further coupling are absent.
4. The gas consists of pure hydrogen.
5. The black hole is nonrotating, and the disk is Newtonian.
6. A copious supply of soft photons is available, so that unsaturated Comptonization dominates the cooling.

The two additional structure equations which, together with equations (3)–(5), determine the disk structure in the hot, inner region, may be now specified. The first equation is a direct consequence of assumption (3):

*electron-ion energy exchange (ion energy balance)*

$$F/h = 3/2 \nu_E \rho k (T_i - T_e) / m_p. \quad (10)$$

In the above equation, the electron-ion coupling rate,  $\nu_E$ , can be approximated by  $\nu_E = 2.4 \times 10^{21} \ln \Lambda \rho T_e^{-3/2}$  (Spitzer 1962), where the Coulomb logarithm  $\ln \Lambda \approx 15$  in the present case. Rapid thermalization by plasma instabilities leading to  $T_e \sim T_i \gtrsim 10^{10} \text{ K}$  is assumed to be absent. Collisionless shock heating, which can equilibrate electron and ion temperatures in a few ion plasma periods (Shapiro and Salpeter 1975) will not be significant when turbulent velocities are subsonic, i.e.,  $\alpha < 1$  (Shakura and Sunyaev 1973). It has been pointed out by Rees (1975) that if the viscosity is too high ( $\alpha \sim 1$ ), then shock heating may be important.

The remaining structure equation expresses the fact that Comptonization is the dominant cooling mechanism in the inner disk:

*inverse (unsaturated) Compton cooling (electron energy balance)*

$$F/h = (4kT_e/m_e c^2) \rho \kappa_{\text{es}} U_r c, \quad \text{i.e., } y = 1, \quad (11)$$

where

$$y \equiv (4kT_e/m_e c^2) \text{Max}(\tau_{\text{es}}, \tau_{\text{es}}^2)$$

is the dimensionless parameter that characterizes Comptonization (see Zel'dovich and Shakura 1969). The radiation energy density,  $U_r$ , appearing above satisfies  $U_r \approx (F/c) \text{Max}(1, \tau_{\text{es}})$ . When bremsstrahlung is the main source of photons, the above expression for Compton cooling of the electrons is not appropriate. In that case our calculations indicate the process will *saturate*; i.e., the energy of a typical photon increases to  $\sim 3kT_e$  by repeated scatterings, at which point further scatterings transfer no net energy from the electrons. *Saturated* Comptonization, characterized by  $y \gg 1$ , can be significant in the inner region of the cool disk model (Shakura and Sunyaev 1973; Lightman and Shapiro 1975). *Unsaturated* Comptonization, given by equation (11), gives  $y \sim 1$  and is appropriate whenever there is a copious source of soft photons in the hot inner region; see § IIIb. The origin of this source in our model and the corresponding spectrum are discussed in § IIIb, c.

Equations (3)–(5), (10), and (11) now comprise a complete set of equations for the five unknown disk structure variables  $\rho$ ,  $h$ ,  $P$ ,  $T_i$ , and  $T_e$ . The solution to the equations are:

$$T_e = (7 \times 10^8 \text{ K}) (M_* \dot{M}_*^{-1} \alpha^{-1} \mathcal{J}^{-1})^{1/6} r_*^{1/4}, \quad (12a)$$

$$T_i = (5 \times 10^{11} \text{ K}) M_*^{-5/6} \dot{M}_*^{5/6} \alpha^{-7/6} \mathcal{J}^{5/6} r_*^{-5/4}, \quad (12b)$$



$$h = (1 \times 10^5 \text{ cm}) M_*^{7/12} \dot{M}_*^{5/12} \alpha^{-7/12} \mathcal{J}^{5/12} r_*^{7/8}, \quad (12c)$$

$$\rho = (5 \times 10^{-5} \text{ g cm}^{-3}) M_*^{-3/4} \dot{M}_*^{-1/4} \alpha^{3/4} \mathcal{J}^{-1/4} r_*^{-9/8}, \quad (12d)$$

$$P = (2 \times 10^{15} \text{ dyn cm}^{-2}) M_*^{-19/12} \dot{M}_*^{7/12} \alpha^{-5/12} \mathcal{J}^{7/12} r_*^{-19/8}. \quad (12e)$$

Important dimensionless quantities which may be computed from the above equations are

$$h/r \sim 0.2 M_*^{-5/12} \dot{M}_*^{5/12} \alpha^{-7/12} \mathcal{J}^{5/12} r_*^{-1/8}, \quad (13a)$$

$$\tau_{\text{es}} \sim 2 M_*^{-1/6} \dot{M}_*^{1/6} \alpha^{1/6} \mathcal{J}^{1/6} r_*^{-1/4}, \quad (13b)$$

$$T_e/T_i \sim 1 \times 10^{-3} M_* \dot{M}_*^{-1} \alpha \mathcal{J}^{-1} r_*^{3/2}. \quad (13c)$$

We observe from equation (12a) that the computed value of  $T_e$  is near  $\sim 10^9$  K and is nearly independent of the radius,  $M$ ,  $\dot{M}$ , and  $\alpha$  throughout the two-temperature domain. Equation (13a) indicates that this region is geometrically thick, with  $1 > h/r \gtrsim 0.2$ , due to the high value of the ion temperature. The ratio,  $A_{\text{ff}}$ , of inverse Compton cooling to free-free emission in the two-temperature domain is

$$A_{\text{ff}} = \frac{F/h}{\Lambda_{\text{ff}}} = (8 \times 10^3) M_*^{-7/6} \dot{M}_*^{7/6} r_*^{-7/4} \alpha^{-5/6} \mathcal{J}^{7/6} \gg 1. \quad (14)$$

Thus, Comptonization is far more efficient than bremsstrahlung alone as a cooling mechanism.

The above equations apply to a Newtonian disk model. Since we assume that the black hole is nonrotating, general-relativistic corrections are not significant.

We have used the thin-disk approximation ( $h/r \ll 1$ ) to derive this model; clearly, this approximation is no longer strictly valid. The theory of *thick* accretion disks (see Bardeen 1972) unfortunately has not yet been worked out. We believe that the thin-disk equations are still valid to a factor of 2 in the present model and that the conclusions we draw are substantially unaffected, as long as the disk is not so thick ( $h/r \sim 1$ ?) that a substantial amount of matter is blown radially into the hole or vertically to infinity by pressure gradients; whether this is possible in our model is an open question.

### b) The Emission Spectrum

The formation of X-ray spectra by inverse Compton scattering has been discussed by Illarionov and Sunyaev (1972), and Felten and Rees (1972) (for the case of a thermal bremsstrahlung source); and by Zel'dovich and Shakura (1969) (for the case of a soft photon source). It is an essential assumption of our model that there exists for the two-temperature region a copious soft (X-ray) photon source, much stronger than bremsstrahlung, cyclotron, or double Compton scattering. In this situation cooling takes place under the condition  $y \approx 1$  ("unsaturated Comptonization"; see eq. [11] above) and  $A \gg 1$ , where  $A$  is the energy enhancement factor due to Comptonization for arbitrary emission processes. However, the method of Zel'dovich and Shakura is inapplicable to the case  $y \approx 1$ ,  $A \gg 1$  because of a subtle but crucial point: Most of the emitted energy is carried by those few photons which remain in the disk for many scatterings (even though  $\tau_{\text{es}} \sim 1$ ) and which thereby become especially hard. Therefore, it is essential to model photon transport, not by a mean number of scatterings before escape, but by a mean probability of escape per scattering. The steady-state Kompane'ets equation (Kompane'ets 1956; Weymann 1965; Cooper 1971) governing the spectrum then takes the form

$$0 = \frac{1}{E^2} \frac{d}{dE} \alpha(E, T_e) \left[ n + kT_e \frac{dn}{dE} \right] + S(E) - \beta(E)n, \quad (15)$$

where

$$n = \text{photon occupation number} \left( I_\nu = \frac{2h\nu^3}{c^2} n \right), \quad \text{assumed isotropic};$$

$$E = \text{photon energy (keV)};$$

$$kT_e = \text{electron temperature (keV)};$$

$$S(E) = \text{photon source (per state per Thomson scattering time)};$$

$$\beta(E) = \text{mean rate of photon escape from the disk, per Thomson scattering time, per photon in the disk} \\ \approx \text{Min}(\tau_{\text{es}}^{-1}, \tau_{\text{es}}^{-2}); \text{ here } \tau_{\text{es}} \text{ is computed from the total Klein-Nishina cross section. Note that}$$

$$\beta(0) \equiv (4kT_e/m_e c^2)/y;$$

$$\alpha(E, T_e) = \frac{E^4}{m_e c^2} [1 + f(T_e)/(1 + 0.02E)][1 + 4.2 \times 10^{-3}E + 9 \times 10^{-6}E^2]^{-1},$$

where

$$f(T_e) = 2.5\theta + 1.875\theta^2(1 - \theta), \quad \text{and} \quad \theta \equiv kT_e/m_e c^2.$$

In the expression for  $\alpha$ , the factors in square brackets are the special-relativistic corrections, due to Cooper (1971). These corrections are accurate for  $E \lesssim 1$  MeV,  $kT_e \lesssim 100$  keV. We have neglected the stimulated scattering term, proportional to  $n^2$ , in equation (15); this term is unimportant in the X-ray regime under present conditions.

When there exists a copious supply of soft photons [represented by a source term  $S(E)$  in eq. (15)] which vanishes above some soft energy  $E_s$ , the shape of  $n(E)$  for  $E > E_s$  is completely independent of the details of  $S(E)$ . For  $E > E_s$ ,  $E \ll kT_e$ ,  $n(E)$  is approximately self-similar:

$$n(E) \propto E^m, \quad \text{where} \quad m = -\frac{3}{2} - \left[ \frac{9}{4} + \frac{4}{y(1+f)} \right]^{1/2}. \quad (16)$$

For  $y \approx 1$ , equation (16) gives an energy spectrum  $I_\nu \propto E^3 n \propto E^{-1}$ . For  $E \gtrsim kT_e$ , the spectrum falls roughly like  $\exp(-E/kT_e)$ . When the relativistic corrections to  $\alpha$  and  $\beta$  are omitted (valid for  $kT_e \lesssim 25$  keV), equation (15) can be solved exactly for the special case  $y = 1$ :

$$I_\nu \propto E^{-1} e^{-x} \left( 1 + x + \frac{1}{2} x^2 + \frac{1}{6} x^3 + \frac{1}{24} x^4 \right), \quad (17)$$

where  $x \equiv E/kT_e$ . This solution is not very accurate under present conditions, but it well illustrates the qualitative shape of the spectrum. In general, equation (15) must be solved numerically; we have used the scheme of Chang and Cooper (1970) for the numerical work.

Equation (15) may not strictly apply in the real world because (a) the Fokker-Planck approximation (diffusion approximation to photon scattering in  $E$ -space) may break down, (b) the simple, probabilistic rate  $\beta$  may be an insufficient model of photon escape, (c)  $n$  may deviate strongly from isotropy at high  $E$ . All these effects are difficult to estimate; we suspect (c) to be the most significant. If these effects are important, they will have strongest effects on the spectrum at  $E > 100$  keV (deviation from exponential spectrum), or at  $E_s < E \lesssim 2E_s$  (deviation from self-similar spectrum).

We can now understand the cooling condition  $y \sim 1$  (eq. [11]) and examine its sensitivity to the soft photon luminosity  $L_s$ . The shape of  $S(E)$  and the precise value of  $T_e$  make little difference; let us choose a delta-function

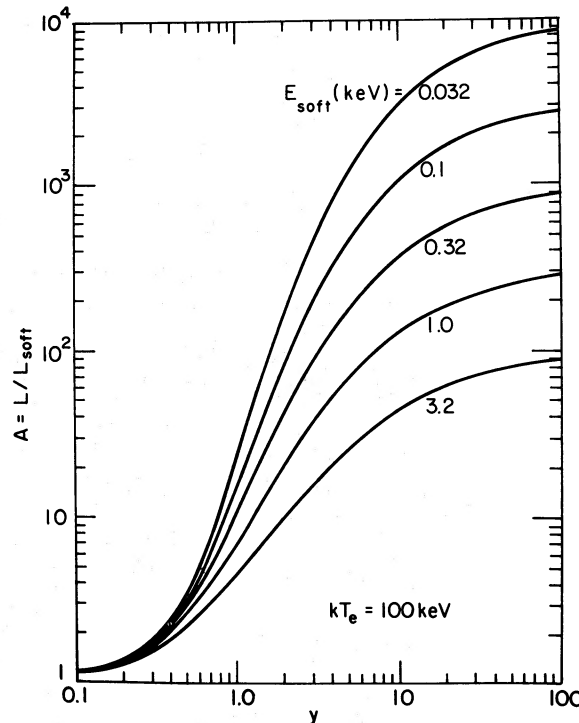


FIG. 1.—Energy enhancement factor  $A$  for Comptonization of a soft photon source, as a function of the parameter  $y \equiv (4kT_e/m_e c^2) \text{Max}(\tau_{\text{es}}, \tau_{\text{es}}^2)$  and of the characteristic energy  $E_{\text{soft}}$  of the source. Electron temperature  $kT_e \equiv 100$  keV ( $T_e = 1.16 \times 10^9$  K) and source shape  $S(E) \propto \delta(E - E_{\text{soft}})$ , which are representative, are adopted.

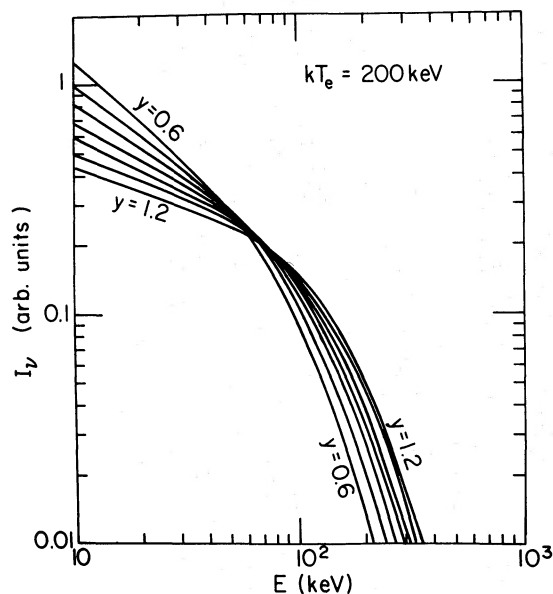


FIG. 2.—Spectral shapes of a Comptonized soft photon source, for photon energy  $E > 10$  keV, and for  $\gamma$  in the range  $0.6 \leq \gamma \leq 1.2$  with steps  $\Delta\gamma = 0.1$ . Each curve gives the spectral energy density  $I_\gamma$ , normalized to the same total luminosity  $L_{>10}$  above 10 keV. Shapes are not very dependent on adopted electron temperature  $kT_e = 200$  keV ( $T = 2.32 \times 10^9$  K) and are independent of soft source shape  $S(E)$  provided  $S(E)$  cuts off below 10 keV (and assuming the approximations that underlie equation 15 hold; see § IIIb). In our model, these changes in shape could be caused by changes in the luminosity  $L_s$  of the soft source,  $4.5 \lesssim L_{>10}/L_s \lesssim 41$ , if  $E_s = 0.1$  keV.

at  $E_s$  for  $S(E)$  and  $kT_e = 100$  keV ( $T_e = 1.16 \times 10^9$  K). Since the total luminosity  $L$  is essentially fixed by observation,  $L_s$  is determined by the energy enhancement factor  $A \equiv L/L_s$ .

Values of  $A$  as a function of  $E_s$  and  $\gamma$  are presented in Figure 1, from numerical integrations of equation (15). For small  $E_s$ ,  $A(\gamma)$  rises very steeply in the region  $\gamma \sim 1$ , much more steeply than  $e^\gamma$ . This steep rise is due to the rare photons that remain in the disk for many scatterings and become hard. We can understand qualitatively the shape of the curves  $A(\gamma)$  through this derivation, which ignores the relativistic corrections to  $\alpha$  and  $\beta$ : To express conservation of energy, we multiply equation (15) by  $E^3$  and integrate over  $E$ . The result can be solved for  $\gamma$  to give the relation

$$\gamma = \frac{1 - A^{-1}}{1 - \langle E \rangle / 4kT_e},$$

where  $\langle E \rangle \equiv \int E^4 ndE / \int E^3 ndE$  is the intensity-weighted mean spectral energy. This relation explains the three regimes as  $\gamma$  ranges from 0 to  $\infty$ , which are apparent in Figure 1: (a) *Negligible Comptonization*. The emergent spectrum is essentially that of the input spectrum  $S(E)$ ,  $\langle E \rangle / 4kT_e \ll 1$ ;  $A \approx 1$ , so numerator  $\ll 1$ , hence  $\gamma \ll 1$ . (b) *Unsaturated Comptonization*. As  $\gamma \rightarrow 1$ , the spectrum remains soft,  $\langle E \rangle / 4kT_e \ll 1$ , so the denominator  $\approx 1$ . This gives  $A^{-1} \ll 1$ , i.e.,  $A$  becomes large. (c) *Saturated Comptonization*. Eventually  $A$  increases to  $\sim kT_e/E_s$ , so most photons become hard, and  $\langle E \rangle / 4kT_e$  becomes finite in the denominator, driving  $\gamma$  up. Finally spectrum approaches a Wien spectrum  $n \propto e^{-E/kT}$ , for which  $\langle E \rangle = 4kT_e$ , so  $\gamma \gg 1$ , with  $A \rightarrow 3kT_e/E_s$ .

In nature, of course, the above calculation is reversed. The soft luminosity  $L_s$  is determined by the thermal structure of the disk. As long as the soft photon source is sufficiently copious  $E_s/kT_e \ll L_s/L \ll 1$ , Figure 1 shows that  $\gamma \sim 1$ , in the regime of unsaturated Comptonization. The value of  $\gamma$  is well buffered near 1 against large excursions in  $L_s$ ; e.g., for  $E_s = 0.1$  keV,  $L_s$  can range over a factor of 100 while  $\gamma$  stays between 0.5 and 2.5. (In actuality, there may well be feedback from conditions in the disk to  $L_s$  which further stiffens the buffering.) Therefore, the structure of the disk is very insensitive to changes in  $L_s$  in the regime  $\gamma \sim 1$ , as long as  $E_s$  is small.

The predicted spectral shape, however, is sensitive to changes in  $\gamma$ , and therefore is slightly sensitive to changes in  $L_s$ . It is the self-similar slope below  $\sim kT_e$  that is most sensitive to changes in  $\gamma$ ; see equation (16). We present in Figure 2 computed spectral shapes for the range  $0.6 \leq \gamma \leq 1.2$ , for adopted values  $kT_e = 200$  keV ( $T_e = 2.32 \times 10^9$  K) and  $E_s = 0.1$  keV, with  $S(E) = \delta(E - E_s)$ . [The precise value of  $T_e$  makes little difference; the value of  $E_s$  or the shape of  $S(E)$  makes no difference at all to the shape as long as  $E_s < E$ .] These spectra are all normalized to have the same total luminosity  $L_{>10}$  above  $E = 10$  keV (known from observations in the case of Cyg X-1). At  $E_s = 0.1$  keV, this range of spectra corresponds to a range of  $A$ ,  $9.1 \leq A \leq 48.5$ ; or a range of the ratio of observed energy  $L_{>10}$  to soft energy  $L_s$ ,  $4.5 \leq L_{>10}/L_s \leq 41.3$ . These ranges would be smaller if  $E_s$  were greater.

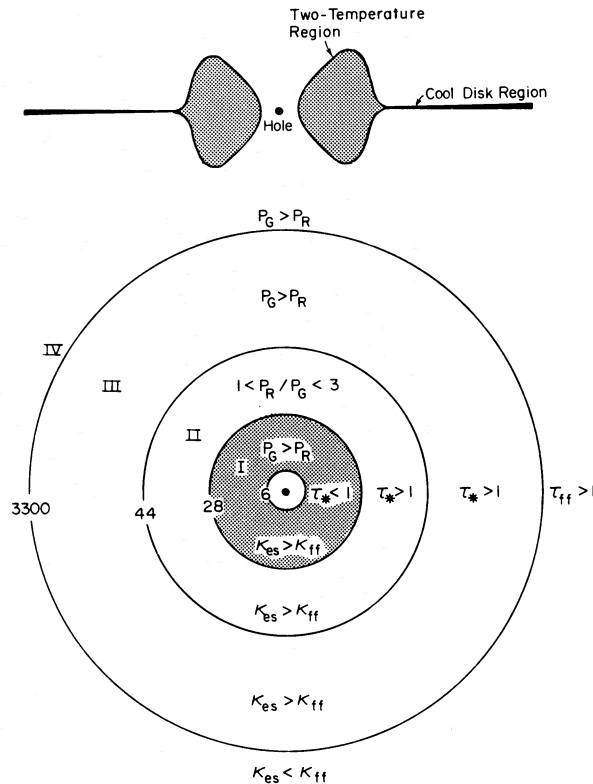


FIG. 3.—(a) (top) A side view (to scale) of the inner portions of an accretion disk around a nonrotating black hole. For this model,  $M = 10 M_{\odot}$ ,  $\alpha = 0.1$ ,  $M = 7 \times 10^{17} \text{ g s}^{-1}$ ,  $E_s = 0.5 \text{ keV}$ . The observed X-rays ( $E > 1 \text{ keV}$ ) are produced in the hot, bloated, two-temperature region, extending from  $90 \text{ km} \leq r \leq 410 \text{ km}$  and joining onto the thin cool disk region. (b) (bottom) A top view (not to scale) of the accretion disk for the same model parameters as Fig. 3a, illustrating the various disk regions. Optical depths, pressures, and opacities are denoted by  $\tau$ ,  $P$ ,  $\kappa$ , respectively (see text). Region IV is the cool disk “outer region,” which generates in each radial annulus a blackbody spectrum. Regions III and II are the cool disk “middle” and “inner” regions, respectively, which produce modified (by scattering) blackbody spectra at surface temperatures  $T_e \lesssim 3 \times 10^6 \text{ K}$ . Region I is the “two-temperature inner region,” where  $T_e \sim 2 \times 10^9 \text{ K}$ ,  $T_i \sim 1-2 \times 10^{11} \text{ K}$ , and the spectra are produced by unsaturated Comptonization (see text). Radial boundaries of the regions are in units of  $GM/c^2 = 14.7 \text{ km}$ .

Since we do not know  $L_s$ , we must make some assumption in building our model. We just choose  $y \equiv 1$  throughout. In light of the preceding discussion, this choice is well justified for determining the disk structure, but it is to some extent arbitrary for determining the precise spectral shape. This point will be discussed in § IVa.

### c) Origin of the Soft Photons

The spectral energy curve given by equation (15) with  $y \sim 1$  is valid in the hot region of the disk for  $E > E_s$ , whenever there exists a copious supply of soft photons with energy in the range  $50 \text{ eV} \lesssim E_s \lesssim 5 \text{ keV}$ . The lower limit to  $E_s$  is determined by blackbody emission, since, whatever the soft photon source, it cannot produce more photons than a blackbody radiating at the electron temperature  $T_e$  in the hot (nearly isothermal) zone. The intersection of a blackbody curve at  $T_e \sim 10^9 \text{ K}$  with  $I_\nu$  given by equation (15) (normalized to fit the observed spectrum shown in Fig. 3) occurs at 50 eV. Hence, Comptonization of photons softer than 50 eV cannot generate the observed hard X-ray flux. The upper limit to  $E_s$  is also established by the observations, since, above  $\sim 5 \text{ keV}$ , the spectrum given by equation (15) with  $y = 1$  fits the observed points quite well. Since the solution is only valid for  $E > E_s$ , the close fit requires  $E_s < 5 \text{ keV}$ .

With these limits on  $E_s$  we can eliminate thermal cyclotron emission as a significant soft photon source in the hot, inner region. The maximum magnetic field strength in the disk occurs if the magnetic viscosity is comparable to the turbulent viscosity, in which case  $B \sim 10^7$  gauss in the inner regions (Shakura and Sunyaev 1973; Eardley and Lightman 1975). The maximum cyclotron frequency is then  $h\nu_H \sim 0.1 \text{ eV}$ , which is far below the lower limit on  $E_s$ . High-harmonic cyclotron emission above 50 eV ( $n \gtrsim 500$ ) is far too inefficient, even when  $T_e \sim 10^9 \text{ K}$ .

Equation (14) eliminates thermal bremsstrahlung as a strong, soft photon source. Double Compton scattering can likewise be eliminated.

One source of soft X-rays is the cool ( $T_e \sim 10^6 \text{ K}$ ) region of the disk surrounding the hot, inner portion. A substantial flux of soft photons with energies near  $\sim 0.5 \text{ keV}$  impinge upon the hot, inner zone whenever  $h/r \sim 1$



( $\alpha \sim 0.1$ ). We have computed the fraction of the flux emitted in the cool outer regions of the disk which strikes the two-temperature inner region, assuming that the soft photon flux is emitted with a cosine limb-darkening law (approximately valid for a scattering atmosphere; see Chandrasekhar 1950). We find that for model parameters appropriate for Cyg X-1, the ratio  $A$  of the total outgoing energy flux from the hot, inner region to the incident soft energy flux from the cool disk is, typically,  $\sim 10$  for  $\alpha \sim 0.1$ . Figure 1 shows that  $A \sim 10$  under these conditions is consistent with  $\gamma \sim 1$  and  $E_s \sim 0.5$  keV; hence the model is self-consistent.

There may be additional soft photon sources in the inner region. One strong possibility includes emission from random high density, low temperature clumps in pressure and thermal equilibrium with the hot plasma, which form in the inner region due to the secular instability (Lightman 1974b). If the clumps have a size  $d \lesssim r$ , the energy of a typical soft photon should peak near  $E \gtrsim kT_{\text{eff}} \sim 0.5$  keV. We have not ruled out the possibility of soft photon illumination from the infalling gas within the region  $2m < r < 6m$  ( $m = GM/c^2$ ) prior to its capture by the black hole.

#### d) Formation of the Two-Temperature Domain

We have demonstrated above that a new two-fluid solution to the disk structure equations can be found which differs considerably from the radiation-pressure dominated, optically thick inner region of the cool disk model. We now suggest that the secular instability (Lightman and Eardley 1974; Lightman 1974b) which probably occurs within the cool disk inner region will quickly drive the disk from a cool state ( $T_e \sim 10^6$  K) to the hot, two-fluid state ( $T_e \sim 10^9$  K) in this region.

The onset of the secular instability occurs at the radius where  $\partial W(r, \Sigma)/\partial \Sigma$  changes sign; here  $W$  is vertically integrated viscous stress and  $\Sigma$  is surface density (Lightman and Eardley 1974; Lightman 1974a, b). To avoid the instability in the inner region, the derived quantity  $\alpha(\Sigma, r) = W/2hP$  would have to obey  $\partial \ln \alpha / \partial \ln \Sigma < -1$  when  $P_R \gg P_G$  (here  $P_R$  = radiation pressure,  $P_G$  = gas pressure), which does not seem likely. Consequently, the instability will set in at a radius where  $P_R \approx P_G$  (near the outer boundary of the inner region). For instance, for the traditional law  $\alpha = \text{const.}$ , one has for the cool disk, the relation

$$\frac{\partial W}{\partial \Sigma} = \frac{5P_G + 2P_R}{3P_G - 2P_R}. \quad (18)$$

Hence the instability just occurs when

$$P_R = \frac{3}{2} P_G. \quad (19)$$

Using the "cool disk" values for  $P_R$  and  $P_G$ , this condition occurs at the radius  $r_0$  satisfying the relation

$$r_{0*}^{21/8} \mathcal{J}^{-2}(r_0) \approx 1 \times 10^4 \alpha^{1/4} M_*^{-7/4} \dot{M}_*^2. \quad (20)$$

Thus, the hot, two-temperature domain will lie just within the cool disk inner region and will exist whenever the inequality

$$\alpha^{1/4} \dot{M}_*^2 M_*^{-7/4} \gtrsim 0.6$$

is satisfied. (This criterion applies to a nonrelativistic disk. For a fully relativistic disk, set  $\beta = \frac{2}{3}$  in eq. [C1] of Eardley and Lightman 1975.)

The important feature of equation (18) is not this precise criterion for the location of the sign change, which depends on the special assumption  $\alpha = \text{const.}$ , but the fact that the sign changes via a *pole* rather than a zero, which seems to be a general feature. This suggests that the onset of instability is sudden and violent, and that the transition zone between the inner region of the cool disk and the hot, two-temperature region is a narrow region ( $\Delta r/r \ll 1$ ) in which the disk effectively undergoes a "phase change" on the thermal time scale, as elements of the disk enter the "no-solution region" for cool-disk structure (Lightman 1974a).

Our predicted spectrum is quite insensitive to the precise criterion for onset of instability, because the two-temperature region is nearly isothermal (cf. eq. [12a]). In the numerical calculations of § IV, a slightly more conservative criterion for instability, namely,  $P_R = 3P_G$ , has been used.

We note that the hot, two-temperature solution is a valid solution for disk structure outside the inner region as well as within. A real disk might well choose to be in a hot state rather than a cool one, even outside the inner region, for reasons other than those considered here. This possibility was pointed out and discussed by Pringle *et al.* (1973) (although their hot state differs considerably from ours).

#### e) The Modified Accretion Disk Model

We have incorporated the two-fluid disk domain in a modified disk model for Cyg X-1. The "outer" and "middle" regions of the cool disk (see Shakura and Sunyaev 1973; Novikov and Thorne 1973) describe the outer portions of the modified disk model. The inner region of the cool disk, whose outer boundary lies at the point where

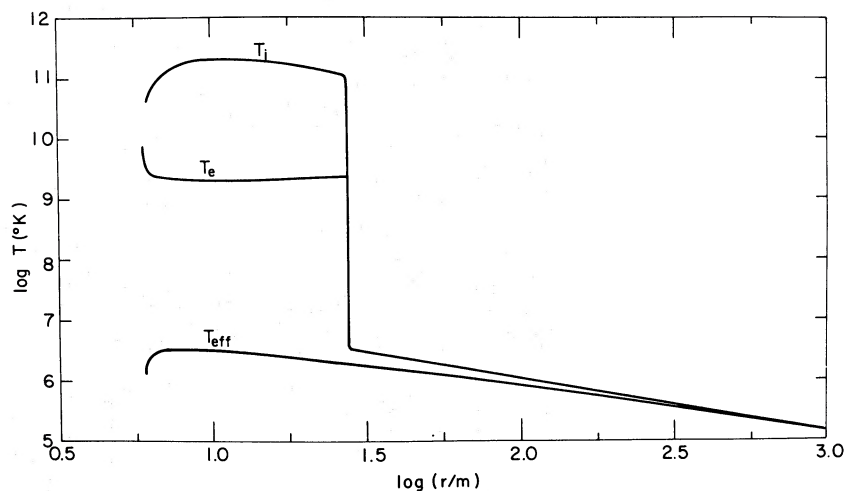


FIG. 4.—Temperature profile of the emitting layers of the identical disk illustrated in Fig. 3. The ion, electron, and effective temperatures ( $T_i$ ,  $T_e$ , and  $T_{\text{eff}}$ , respectively) are plotted against the radial coordinate measuring distance from the central black hole. The “two-temperature inner region” extends from the inner edge of the disk at  $r_i = 6m$  to  $r = 28m$ , where  $m \equiv GM/c^2 = 14.8$  km.

$P_R = P_G$ , extends inward to the radius  $r_0$ , where  $P_R = 3P_G$ . This radius now marks the outer boundary of the “two-temperature inner region,” which then extends inward to the innermost stable circular orbit  $r = r_i = 6GM/c^2$ . The modified disk is therefore identical to the cool disk for  $r \geq r_0$  but is described by the two-temperature structure equations for  $r < r_0$ .

Results of numerical calculations of the emergent continuous radiation spectrum from the entire accretion disk are discussed in the following section. The disk is divided into concentric rings, and the physical variables and emergent spectrum are determined for each ring. For  $r \geq r_0$ , we compute a model atmosphere in each ring from the known surface gravity,  $g(r)$ , and total energy flux  $F(r)$  (see Lightman and Shapiro 1975 for details). For  $r \leq r_0$ , the spectrum in each ring is determined by equation (15) with  $y = 1$ . The total spectrum is then obtained by summing the contributions from each ring.

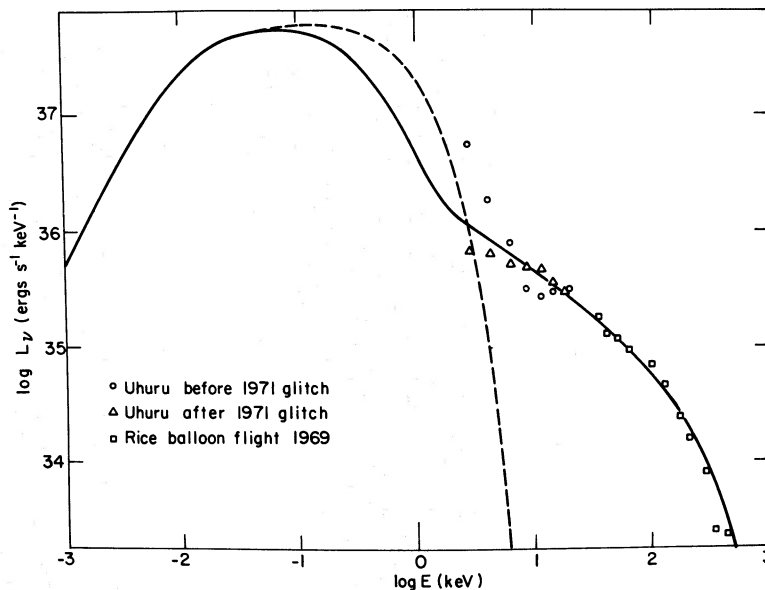


FIG. 5.—Comparison of observed and theoretical spectra for Cyg X-1. The solid curve gives the predicted spectrum of the two-temperature disk model for the same parameters as Figs. 3–4, with  $y \equiv 1$ . The dashed curve gives the predicted spectrum of the previous “cool disk” model for the same values of  $M$ ,  $\dot{M}$ ,  $\alpha$ . The 1969 measurements above 100 keV are uncertain to within factors of  $\sim 2$ , but error bars have been omitted in the figure for simplicity. A distance of 2.5 kpc to Cyg X-1 has been assumed in plotting the data.

TABLE 1  
SPECTRAL PROPERTIES OF THE TWO-TEMPERATURE DISK MODEL

$M$ ( $M_{\odot}$ )	$\dot{M}$ ( $\dot{M}_B$ ) <sup>*</sup>	$\alpha$	$E_s$ (keV)	$L$ ( $10^{37}$ ergs s <sup>-1</sup> )	$r_0$ (100 km)	$L_{r_0}/L$	$T_{e,\max}$ ( $10^9$ K)	LUMINOSITY ( $10^{37}$ ergs s <sup>-1</sup> ) (keV range)				
								(< 0.1)	(0.1–3.0)	(3.0–10)	(10–100)	(> 100)
Observations <sup>†</sup> of Cygnus X-1								...	...	0.9	1.2	0.5
5.....	0.065	0.1	0.5	4.1	3.1	0.68	2.3	0.23	1.5	0.41	1.2	0.54
10.....	0.041	0.1	0.5	5.1	4.1	0.56	2.4	0.42	2.1	0.44	1.3	0.62
10.....	0.041	1.0	0.5	5.1	5.6	0.65	1.7	0.41	1.6	0.46	1.8	0.84
10.....	0.035	0.1	5.0	4.4	3.4	0.48	2.3	0.38	1.8	0.34	1.3	0.62
20.....	0.028	0.1	0.5	7.0	5.6	0.41	2.3	0.81	3.6	0.43	1.3	0.65
20.....	0.027	0.1	0.5	6.8	5.3	0.38	2.3	0.80	3.7	0.36	1.1	0.55

<sup>\*</sup>  $\dot{M}_B = 1.67 \times 10^{18} (M/M_{\odot}) \text{ g s}^{-1}$ .

<sup>†</sup> Haymes and Harnden 1970; Schreier *et al.* 1971. Tabulated values give the pre-1971 glitch observations and assume a distance of 2.5 kpc.

#### IV. NUMERICAL RESULTS AND DISCUSSION

Results of numerical calculations of the disk structure and emission spectrum are summarized in Figures 3–5 and Table 1. Figure 3 illustrates the geometrical profile and different physical regimes characterizing an accretion disk around Cyg X-1 for a typical model. Figure 5 gives the theoretical spectrum for the same model, together with some representative observed spectra of Cyg X-1 (Haymes and Harnden 1970; Schreier *et al.* 1971), and the predicted spectrum for the cool disk model. Figure 4 gives the ion, electron, and effective temperature profiles in the hot disk model for the same model depicted in Figure 3. The results for different model parameters, all chosen to fit the observations of Cyg X-1, are summarized in Table 1. It is clear from Figure 5 and Table 1 that excellent agreement between the theoretical spectrum and observations can be achieved for a suitable choice of model parameters.

The spectral shape for  $E > E_s$  is specified by equation (15) with  $\gamma = 1$  and reproduces the observed self-similar shape,  $I_{\nu} \propto \nu^{-1}$ , for  $E < kT_e$ , independent of other model parameters. The two remaining features of the spectrum are (1) the location of the “knee” at  $E \sim kT_e$  (observed near 125 keV) and (2) the total integrated luminosity above 3 keV ( $\sim 3 \times 10^{37}$  ergs s<sup>-1</sup> for an assumed distance of 2.5 kpc [Bregman *et al.* 1973]). The first condition is satisfied whenever  $T_e \sim 1\text{--}2 \times 10^9$  K, a result which follows from our model, almost independently of parameters (cf. eq. [12a]). The second condition determines the accretion rate,  $\dot{M}$ , for a given  $\alpha$  and given black-hole mass  $M$ . The integrated luminosity from the inner edge of the disk to  $r_0$  is

$$L_{r_0} = [1 + 2(\frac{1}{6}r_{0*})^{-3/2} - 18/r_{0*}] \dot{M} c^2 / 12. \quad (21)$$

We assume that most of the radiation generated in the two-temperature inner region is observed ( $E \geq 3$  keV). Employing equation (20) to find  $r_{0*}$  as a function of  $\dot{M}$  for a given  $M$  and  $\alpha$ , the condition  $L_{r_0} \sim 3 \times 10^{37}$  ergs s<sup>-1</sup> yields

$$\left[ 1 + 2 \left( \frac{r_{0*}}{6} \right)^{-3/2} - \frac{18}{r_{0*}} \right] r_{0*}^{21/16} \left[ 1 - \left( \frac{r_{0*}}{6} \right)^{-1/2} \right]^{-1} = 2.8 \times 10^2 \lambda, \quad (22)$$

where  $\lambda \equiv (\alpha M_*^{-7})^{1/8}$ . Since  $\lambda$  is insensitive to  $\alpha$ ,  $r_{0*}$  and  $\dot{M}$  are uniquely determined for a given  $M$ , by equations (20) and (22). These values are listed in Table 1. If the soft photons discussed in § IIIb have energies  $E_s \ll 1$  keV and some of the Comptonized radiation of the two-temperature inner region comes out in the low-energy ( $E < 3$  keV) unobserved portion of the spectrum, then the coefficient in front of  $\lambda$  in equation (22) must be increased. The last two entries in Table 1 indicate how sensitive the value of the emitted luminosity above 10 keV is to the mass accretion rate.

The parameter  $\alpha$  is constrained by the model to lie within the range  $0.05 < \alpha < 1$ . The lower bound is set by the requirement that  $h/r < 1$  for an accretion disk. The upper limit ensures that collisionless shock heating, which can bring about a rapid equipartition of ion and electron thermal energy, will not occur (see § IIIa). Since the shape of the disk surface in the hot, inner region depends on  $\alpha$  (see eq. [12c]), a determination of the polarization properties of the hard X-rays originating from the region may constrain  $\alpha$  further (See Lightman and Shapiro 1975).

The thermal instability discussed by Pringle *et al.* (1973), which operates when bremsstrahlung is the photon source in an optically thin gravitationally confined gas, probably is not present in our model. The source of soft photons, which subsequently cool the two-temperature inner region, is presumably thermally uncoupled from the hot optically thin gas.

### a) Long-Term Variations in the Spectrum

As indicated in Figure 3, a sudden change in the soft X-ray spectrum observed by *Uhuru* ( $2 \text{ keV} < E < 20 \text{ keV}$ ) occurred in 1971.<sup>1</sup> It is not clear whether the hard spectrum was also different after 1971. We have not attempted to fit the postglitch spectrum, because hard X-ray ( $E \gtrsim 100 \text{ keV}$ ) observational data is more abundant before 1971.

Besides these major glitches, considerable variations in spectral shape have been reported by observers throughout the history of Cyg X-1 (for references and discussion, see Thorne and Price 1975). In particular, the slope  $m$  of the energy spectrum,  $I_\nu \propto E^{-m}$ , for roughly the range  $10 \text{ keV} < E < 100 \text{ keV}$ , has been reported from  $m = 0.5$  to  $1.0$ ; and the variability seems to be real. Although we will not attempt a proper evaluation in this paper, we suggest that our model can accommodate these changes in  $m$  by changes in  $\gamma$  in the region  $\gamma \sim 1$ , the immediate cause of which would be changes in the soft photon source. To fit the data of Haymes and Harnden, we chose  $\gamma = 1$ . Figure 2 presents a sequence of spectral shapes for  $0.6 \leq \gamma \leq 1.2$  that in fact roughly spans the reported range of slopes. The flatter slopes are more deficient in soft photons in our model. In this regard, we note that the observable soft component of the flux seems to have been small or absent during 1971–1975, and during this time the slope  $m$  seems to have been nearly constant at the flat value  $m \approx 0.5$  (Rothschild 1975). This coincidence suggests that there may be a connection between the observed soft flux and the theoretical one that we require.

### b) Gamma Luminosity

As is well known, an ion gas at  $kT_i \gtrsim 100 \text{ MeV}$  can develop a significant luminosity  $L_\gamma$  for  $\gamma$ -rays,  $10 \lesssim E \lesssim 100 \text{ MeV}$ , through  $\pi^0$  production. Dahlbacka *et al.* (1974) have pointed out that spherical accretion onto an isolated black hole might thereby produce  $L_\gamma \approx 10^{22} \text{ ergs s}^{-1}$ ; this low luminosity is primarily a result of the notorious inefficiency of spherical accretion onto a hole. Our two-temperature disk offers the possibility of a much brighter  $\gamma$ -ray source. In the present model, with a nonrotating hole,  $T_i$  is just not high enough ( $kT_{i,\text{max}} \sim 30 \text{ MeV}$ ), essentially because of the small binding energy of the innermost stable orbit ( $\sim 60 \text{ MeV}$  per baryon). We have made preliminary estimates for the case of a rapidly rotating black hole, for which the binding energy is greater ( $\sim 300 \text{ MeV}$  per baryon); we find some models with  $L_\gamma \sim 10^{37} \text{ ergs s}^{-1} \sim L_X$ . We therefore suggest that rapidly rotating black holes, but not nonrotating ones, can be efficient, compact  $\gamma$ -ray sources, and that this effect may serve as a means to measure the spin of a black hole.

### c) Future Investigations

Future theoretical work on the accretion disk model for Cyg X-1 should correctly model the inner disk as *thick*, should deal with the origin and nature of the soft photon source required by the model (perhaps there are others in addition to the ones mentioned in § III) and should make the model fully relativistic. Our calculations have been for a Newtonian disk around a nonrotating black hole, for which general-relativistic corrections are not significant. General-relativistic effects for accretion onto rapidly rotating holes have been considered by Cunningham (1975) for very thin ( $h/r \ll 1$ ) disk accretion and by Shapiro (1974) for spherical accretion, and will be important for the model considered here. Both general-relativistic effects (redshift, gravitational focusing, and black hole capture of photons) and special relativistic effects (Doppler shifts and forward beaming) will alter the disk structure and, more significantly, the observed radiation spectrum.

It is a pleasure to thank Kip S. Thorne and Richard H. Price for several useful discussions and suggestions and for critically reading the manuscript.

*Note added 1975 October.*— We have learned by personal communication and preprint that J. I. Katz (Institute for Advanced Study, Princeton) has investigated unsaturated Comptonization of a soft photon source in the context of QSO models and has reached conclusions similar to those that we present in § IIIb.

<sup>1</sup> The reverse transition seems to have occurred in 1975 April.

### REFERENCES

- Avni, Y., and Bahcall, J. N. 1975, preprint.  
 Bardeen, J. M. 1973, in *Black Holes*, Les Houches, ed. C. DeWitt and B. DeWitt (New York: Gordon & Breach).  
 Bregman, J., Butler, D., Kemper, E., Koski, A., Kraft, R., and Stone, R. P. S. 1973, *Ap. J. (Letters)*, **185**, L117.  
 Chandrasekhar, S. 1950, *Radiative Transfer* (Oxford: Oxford University Press).  
 Chang, J., and Cooper, G. 1970, *J. Comp. Phys.*, **6**, 1.  
 Cooper, G. 1971, *Phys. Rev. D.*, **3**, 2312.  
 Cunningham, C. T. 1975, preprint.  
 Dahlbacka, G. H., Chapline, G. F., and Weaver, T. A. 1974, *Nature*, **250**, 36.  
 Eardley, D. M., and Lightman, A. P. 1975, *Ap. J.*, **200**, 187.  
 Eardley, D. M., Lightman, A. P., and Shapiro, S. L. 1975, *Ap. J. (Letters)*, **199**, L153.  
 Felten, J. E., and Rees, M. J. 1972, *Astr. and Ap.*, **17**, 226.  
 Haymes, R. C., and Harnden, F. R., Jr. 1970, *Ap. J.*, **159**, 1111.  
 Illarionov, A. F., and Sunyaev, R. A. 1972, *Soviet Astr.—AJ*, **16**, 45.  
 Kompane'ets, A. S. 1956, *Zh. Eksp. Teor. Fiz.*, **31**, 876 (English transl. in *Soviet Phys.—JETP*, **4**, 730 [1957]).  
 Lightman, A. P. 1974a, *Ap. J.*, **194**, 419.  
 ———. 1974b, *ibid.*, p. 429.  
 Lightman, A. P., and Eardley, D. M. 1974, *Ap. J. (Letters)*, **187**, L1.  
 Lightman, A. P., and Shapiro, S. L. 1975, *Ap. J. (Letters)*, **198**, L73.  
 Novikov, I. D., and Thorne, K. S. 1973, in *Black Holes*, Les Houches 1973, ed. C. DeWitt and B. DeWitt (New York: Gordon & Breach).



- Paczynski, B. 1974, *Astr. and Ap.*, **34**, 161.  
 Pringle, J. E., and Rees, M. J. 1972, *Astr. and Ap.*, **21**, 1.  
 Pringle, J. E., Rees, M. J., and Pacholczyk, A. G. 1973, *Astr. and Ap.*, **29**, 179.  
 Rees, M. J. 1975, private communication.  
 Rothschild, R. E. 1975, private communication.  
 Schreier, E., Gursky, H., Kellogg, E., Tananbaum, H., and Giacconi, R. 1971, *Ap. J.*, **170**, L21.  
 Shakura, N. I., and Sunyaev, R. A. 1973, *Astr. and Ap.*, **24**, 337.  
 Shapiro, S. L. 1974, *Ap. J.*, **189**, 343.  
 Shapiro, S. L., and Salpeter, E. E. 1975, *Ap. J.*, **198**, 671.  
 Shvartsman, V. F. 1971, *Astr. Zh.* (English transl. in *Soviet Astr.—AJ*, **15**, 377 [1971]).  
 Spitzer, L., Jr. 1962, *Physics of Fully Ionized Gases* (New York: Wiley).  
 Thorne, K. S., and Price, R. H. 1975, *Ap. J. (Letters)*, **195**, L101.  
 Weymann, R. 1965, *Phys. Fluids*, **8**, 2112.  
 Zel'dovich, Ya. B., and Shakura, N. I. 1969, *Astr. Zh.*, **46**, 225 (English transl. in *Soviet Astr.—AJ*, **13**, 175 [1969]).

*Note added 1975 December.*—We have recently learned from K. S. Thorne that R. A. Sunyaev, N. I. Shakura, and A. F. Illarionov of the Soviet Union have constructed a hot disk model with  $T_e \sim 10^{10}$  K very similar to the two-temperature model discussed here. Because of the decrease in the scattering cross section in the relativistic (Klein-Nishina) domain, a knee in the spectrum still occurs at  $\sim 100$  keV from Comptonization of soft photons.

DOUGLAS M. EARDLEY: Physics Department, Yale University, New Haven, CT 06520

ALAN P. LIGHTMAN and STUART L. SHAPIRO: Center for Radiophysics and Space Research, Cornell University, Ithaca, NY 14853